

Thermohydraulic modelling of a transfer line for continuous flow cryostats

N Dittmar¹, A Weisemann¹, Ch Haberstroh¹, U Hesse¹ and M Krzyzowski²

¹ TU Dresden, Bitzer-Stiftungsprofessur fuer Kaelte-, Kryo- und Kompressorentchnik, Germany

² CryoVac Gesellschaft fuer Tieftemperaturtechnik mbH & Co. KG, Germany

E-mail: nico.dittmar@tu-dresden.de

Abstract. Continuous flow cryostats have to be steadily supplied with the cryogenic cooling agent, e.g. liquid helium (LHe) via a transfer line. The overall setup has to be characterised by a low consumption of the cryogen, determined not only by the cryostat design, but also by the transfer line design. In order to improve the transfer line's performance, i.e. reducing the evaporation losses a thermohydraulic model has been developed to evaluate different transfer line designs. The presented model is validated by experimental data achieved with a transfer line equipped with built-in pressure sensors. This transfer line has been designed in order to examine the related frictional pressure drop. The developed model allows to examine the impact of the hydraulic and the insulation design on the resulting evaporation losses.

1. Introduction

During the analysis of the specific pressure and heat losses of a transfer line used with a continuous flow cryostat (see [1]) it was found that no thermohydraulic model has yet been developed to cover this specific transfer process. Published models, e.g. [2] and [3] cover mainly the transfer of liquid helium (LHe) through rigid transfer lines that supply superconducting magnets. Within the context of a continuous flow cryostat a different transfer process has to be modeled. First of all, the dimension of the transfer line is much smaller compared to that modeled in published papers. Due to the very narrow inner diameter of the transfer line it has to be verified, if correlations for conventional pipe diameters are applicable. Therefore, theoretical results achieved by the homogeneous model (according to [5] and [4]) and for the flow of LHe through a narrow channel [6] and for conventional refrigerants [7] were compared to experimental results. All experimental results were achieved with a transfer line equipped with built-in pressure sensors. The presented thermohydraulic model is used within the design process of a single-channel LHe transfer line aiming lower LHe consumption and operating temperatures.

2. Experimental Setup

The transfer line's pressure drop is measured using an experimental setup similar to a common laboratory setup (see Figure 1). Since a continuous flow cryostat is often characterised by a huge pressure drop, it was excluded in the experiments to reduce the impedance of the overall setup.



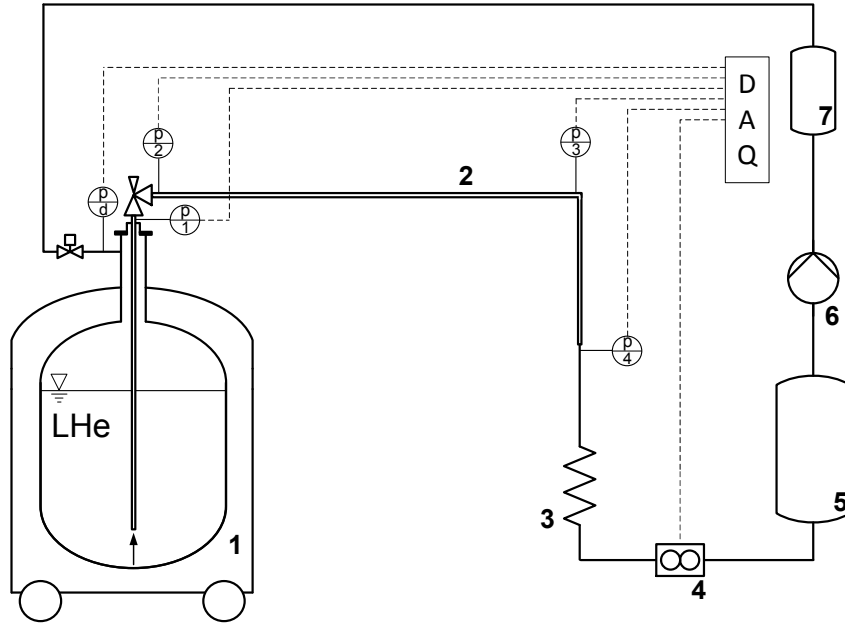


Figure 1. Experimental setup to examine the transfer line's pressure drop; 1: mobile LHe dewar, 2: transfer line, 3: gas heater, 4: mass flow meter, 5: low pressure gas storage, 6: recovery compressor 7: high pressure gas storage.

LHe is feed through the transfer line directly to the helium recovery system of the test facility by pressurizing a mobile dewar (push mode). Once a pressure of 0.15 MPa is reached, the pressurizing valve is shut off and the pressure is relieved while the respective pressure signals and the mass flow rate are acquired. Alternatively, a helium gas pump is installed after the mass flow meter to extract LHe from the mobile dewar (pull mode). The experimental transfer line has a riser length of 1.06 m, a horizontal length of 0.85 m and a vertical length at the cryostat of 0.41 m. The two concentric tubes have an inner diameter of 1.6 mm and an outer diameter of 12 mm in the two vertical sections. The latter increases to 16 mm within the horizontal section. The pressure sensors are located at the end of the riser (p_1), after the needle valve (p_2), at the end of the horizontal section (p_3) and at the transfer line outlet (p_4). If the transfer line is operated in pull mode, then the transfer line is equipped with pressure transmitters having a range of 0 to 0.1 MPa_{abs}. In the case of the push mode the range is 0 to 0.06 MPa_g. All transmitters feature a typical measurement uncertainty of 0.5% FS. The mass flow meter has an accuracy of 2% of the measured value. Remaining LHe is evaporated and the complete flow is warmed up to be stored in gas tanks. A detailed description of the test setup is found in [1].

3. Thermohydraulic model

3.1. Pressure drop correlations

The total pressure drop $\Delta p_{tot} = \Delta p_{fr} + \Delta p_g + \Delta p_{acc}$ is composed of the frictional pressure drop Δp_{fr} , the gravitational pressure drop term Δp_g , and the pressure drop caused by acceleration of the flow Δp_{acc} . The frictional pressure drop of the two-phase flow $\Delta p_{fr,tp}$ is:

$$\Delta p_{fr,tp} = \phi_{L0}^2 \cdot f_{fr} \cdot \frac{G^2 \cdot l}{2 \cdot d_i \cdot \rho_l}, \quad (1)$$

where ϕ_{L0}^2 is the two-phase multiplier, $G = \dot{m}_{tot}/A_i$ the mass flux and f_{fr} the Darcy-Weisbach friction factor [8, 9]. For a rough tube the friction factor is defined as:

$$\frac{1}{\sqrt{f_{fr}}} = -2 \cdot \log_{10} \left(\frac{k_{tube}}{3.7 \cdot d_i} + \frac{2.51}{Re_{L0} \cdot \sqrt{f_{fr}}} \right), \quad (2)$$

with $Re_{L0} = G \cdot d_i / \eta_l$ being the Reynolds number, assuming that the complete flow is in liquid state [10]. The two-phase multiplier for a homogeneous flow as in [4, 5] is:

$$\phi_{L0}^2 = \left(1 + x \cdot \frac{\eta_l - \eta_g}{\eta_g} \right)^{-0.25} \cdot \left(1 + x \cdot \left(\frac{\rho_l}{\rho_g} - 1 \right) \right). \quad (3)$$

The change in elevation is accounted for by: $\Delta p_g = \pm \rho_{tp} \cdot g \cdot \Delta h$, with ρ_{tp} being the mean density of the homogeneous flow [9]. Due to its partly evaporation, the LHe flow is accelerated inside the transfer line, resulting in Δp_{acc} :

$$\Delta p_{acc} = G^2 \cdot \left[\left(\frac{(1-x)^2}{(1-\alpha) \cdot \rho_l} + \frac{x^2}{\alpha \cdot \rho_g} \right)_{out} - \left(\frac{(1-x)^2}{(1-\alpha) \cdot \rho_l} + \frac{x^2}{\alpha \cdot \rho_g} \right)_{in} \right], \quad (4)$$

with α being the void fraction of the homogeneous flow [9].

The above given correlations for the frictional pressure drop are derived from the homogeneous modell. Since the diameter of the process line is only 1.6 mm, pressure drop correlations for LHe flow in narrow channels, i.e. mini- and micro-channels were considered, too. According to [6, 11] the two-phase pressure drop of a LHe flow in a 1.6 mm narrow channel is:

$$\Delta p_{fr,tp} = \Delta p_{fr,L0} \cdot \left[1 + F(x) \cdot \left(\frac{f_{fr,G0} \cdot \rho_l}{f_{fr,L0} \cdot \rho_g} - 1 \right) \right]. \quad (5)$$

with $\Delta p_{fr,L0}$ being the single-phase frictional pressure drop of an assumed all liquid flow. The Factor $F = (\Delta p_{fr,tp} - \Delta p_{fr,L0}) / (\Delta p_{fr,G0} - \Delta p_{fr,L0})$ is a function of the flow quality. The respective correlations can be derived from [6]. An approach proposed by [7] valid for mini- and micro-channels was chosen as third correlation. In the case where both phases are turbulent ($Re > 2000$) the two-phase multiplier is defined as:

$$\phi_{L0}^2 = \left[1 + \frac{C}{X} + \frac{1}{X^2} \right] \cdot (1-x)^{1.75}, \quad (6)$$

$$C = 0.39 \cdot Re_{L0}^{0.03} \cdot \left(\frac{\rho_g \cdot \sigma \cdot d_i}{\eta_g^2} \right)^{0.1} \cdot \left(\frac{\rho_f}{\rho_g} \right)^{0.35} \cdot [1 + 60 \cdot We_{L0}^{0.32} \cdot Bo^{0.78}]. \quad (7)$$

Equation (7) is only valid if the ratio of the heated and the wetted perimeter is unity. Otherwise the boiling number Bo has to be corrected. Factor X^2 is the ratio of $\Delta p_{fr,l} / \Delta p_{fr,g}$. The single-phase pressure drop terms are calculated for the specific mass fluxes, i.e. $G \cdot (1-x)$ and $G \cdot x$, respectively. Detailed information on equations and symbols are presented in [7].

3.2. Heat transfer correlations

The overall heat transfer from the ambience to the LHe flow is composed of radiation heat transfer to the MLI, heat transfer through the MLI, heat conduction along spacers, and convective heat transfer to the LHe flow. Table 1 gives an overview on the heat transfer modes, the respective correlations, and references.

Table 1. Overview of implemented heat transfer modes and correlations.

Mode	Correlation	ID
Radiation	$\dot{Q}_{rad} = C \cdot A_o \cdot \left[\left(\frac{T_{w,o}}{100} \right)^4 - \left(\frac{T_{MLI}}{100} \right)^4 \right]$	(8) [12]
	$C = 5.67 \text{ W(m}^2\text{K}^4) \cdot \left(\frac{1}{\varepsilon_{i,o}} - 1 + \frac{1}{\varphi} + \left(\frac{1}{\varepsilon_{o,i}} - 1 \right) \cdot \frac{A_o}{A_i} \right)^{-1}$	(9) [12]
MLI	$\frac{\dot{Q}_{MLI,rad}}{A_{MLI}} = \frac{5.754 \cdot 10^{-7} \cdot \bar{N}^{2.02} \cdot T_m}{N_S + 1} \cdot (T_{MLI} - T_w) + \frac{1.089 \cdot 10^{-9} \cdot \varepsilon_{Alu} \cdot \varepsilon_{Mylar}}{(\varepsilon_{Alu} + \varepsilon_{Mylar}) \cdot N_S} \cdot (T_{MLI}^{4.67} - T_w^{4.67})$	(10) [13]
	$\dot{Q}_{MLI,cond} = \frac{\lambda_{Alu} \cdot \delta_{Alu} \cdot l}{N_S \cdot \pi \cdot (d_i + \delta_{MLI})} \cdot (T_{MLI} - T_w)$	(11) [12]
Tubeside	$\dot{Q}_{tube} = \frac{T_w - T_B}{R_{tube}}$	(12) [12]
	$R_{tube} = \frac{1}{2 \cdot \pi \cdot l} \cdot \left(\frac{1}{h \cdot r_i} + \frac{1}{\lambda_{tube}} \cdot \ln \frac{r_o}{r_i} \right)$	(13) [12]
Convection	$h_{sp} = 0.023 \cdot Re^{0.8} \cdot Pr^{1/3} \cdot \frac{\lambda}{d_i}$	(14) [14]
Boiling	$h_B = 0.015 \cdot Re^{0.8} \cdot Pr^{1/3} \cdot \frac{\lambda}{d_i}, (x < 0.2; x > 0.8)$	(15)
	$h_B = (X_{tt}^{-0.66} + 1500 \cdot Bo^{0.8}) \cdot h_{B,L0}, (0.2 < x < 0.8)$	(16) [16]
Conduction	$\dot{Q}_{Spacer} = \left[\frac{d_o}{2 \cdot \lambda_{PTFE}} \cdot \ln \left(\frac{d_o}{d_i + 2 \cdot \delta_{MLI}} \right) \right]^{-1} \cdot$	
	$\pi \cdot d_o \cdot \delta_{PTFE} \cdot 0.1 \cdot (T_{amb} - T_w)$	(17) [15]

To calculate the radiation heat transfer the inner and outer tube are regarded as two parallel finite cylinders. The view factor is calculated accordingly (see [12]). Several layers of MLI (single aluminized mylar foil) are applied to the inner tube. Equation (10) by [13] is valid for a layer density \bar{N} greater than 34.3 layers/cm.

The heat transfer coefficient is calculated in accordance with the state of the flow and the dominating heat transfer mode. For a single-phase flow the Dittus-Boelter correlation (equation (14)) is used. During boiling the heat transfer coefficient is calculated using correlations published in [16]. In the low and high quality range ($x < 0.2$; $x > 0.8$) h_B is derived from equation (15) using the liquid ($x < 0.2$) or gaseous properties. Within the intermediate range h_B is a function of the boiling number $Bo = q / (h_{vp} \cdot G)$ and the Lockhart-Martinelli parameter X_{tt} . For a turbulent flow of both phases X_{tt} is defined as [17]:

$$X_{tt} = \left(\frac{\rho_g}{\rho_l} \right)^{0.5} \cdot \left(\frac{\eta_l}{\eta_g} \right)^{0.1} \cdot \left(\frac{1-x}{x} \right)^{0.9}. \quad (18)$$

3.3. Critical heat flux

Due to the very low mass flux during cryostat operation, compared to the overall heat flux, it is appropriate to check if film boiling occurs. This can be checked by comparing the actual heat flux with the critical heat flux (CHF): $q_{cr} = K \cdot G \cdot h_{vp}$. Factor K is a function of the limiting quality x_{lim} . The respective correlations for K are presented in [6]. The limiting quality x_{lim} separates the low quality region (q_{cr} decreases linearly with increasing x) and the high quality region (very low values of q_{cr}). The relation for CHF was derived from experimental data of $0.1 < p < 0.2$ MPa, $80 < G < 320$ kg/(m² s), and over the complete quality range [6].

4. Implemented model

The modeled transfer line is diverted into sections with a length of $l_j \approx 0.1$ m. The process parameters, like pressure or quality, are calculated in an iterative procedure. The respective outlet conditions are derived by the conservations of mass, momentum and energy:

$$\dot{m}_{tot,j} = (1 - x_j) \cdot \dot{m}_{l,j} + x_j \cdot \dot{m}_{g,j}, \quad (19)$$

$$p_{out,j} = p_{in,j} - (\Delta p_{fr,j} + \Delta p_{g,j} + \Delta p_{acc,j}), \quad (20)$$

$$h_{out,j} = h_{in,j} + \frac{\dot{Q}_{tot,j}}{\dot{m}_{tot,j}} - 0.5 \cdot (c_{out,j}^2 - c_{in,j}^2) \pm g \cdot \Delta h_j. \quad (21)$$

The inlet pressure of the entry section is given by the transport vessel pressure increased by the hydrostatic pressure of the liquid level. The overall heat leak per section is defined as:

$$\dot{Q}_{tot,j} = \dot{Q}_{conv,j} = \frac{T_{MLI,j} - T_{B,j}}{R_{tube,j} + R_{MLI,j}} + \dot{Q}_{spacer,j} + \dot{Q}_{valve,j} \quad (22)$$

Thereby, the temperature of the outermost MLI layer T_{MLI} is derived from the radiation heat transfer, $\dot{Q}_{MLI,tot,j} = \dot{Q}_{rad,j}$. In equation (22) the term $\dot{Q}_{conv,j}$ represents the convective heat transfer from the inner wall tube to helium two-phase flow. It is equal to the overall heat leak from the outer wall to the inner tube. The heat leak by the valve is added to the total heat leak at the end of the riser ($z = 1.06$ m). Spacers are considered at $z = 1.01$, 1.2 , and 1.88 m. The heat conductivity of the PTFE spacer material is implemented as temperature dependent. A more thorough description of the thermohydraulic model can be found in [18].

5. Results and discussion

The experimental and theoretical results of the total pressure drop in the riser and the horizontal section are presented in Figures 2 and 3.

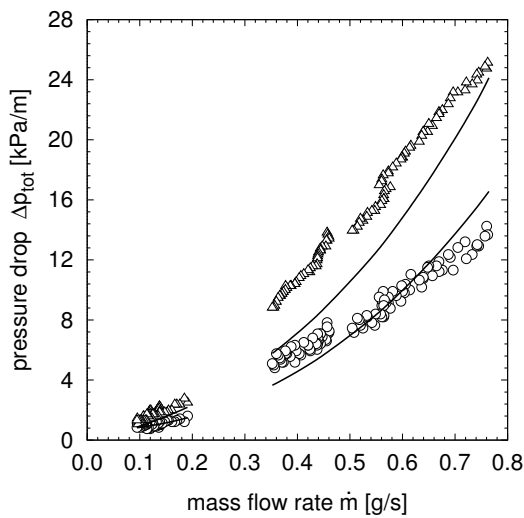


Figure 2. Total pressure drop per unit length of the transfer line; $(p_{dewar} - p_1)_{tot}$ (\circ), $(p_2 - p_3)_{tot}$ (\triangle), homogeneous model (—).

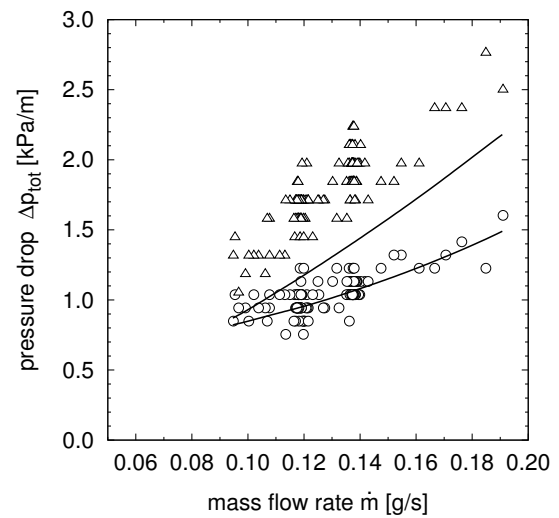


Figure 3. Total pressure drop per unit length in pull mode; $(p_{dewar} - p_1)_{tot}$ (\circ), $(p_2 - p_3)_{tot}$ (\triangle), homogeneous model (—).

It is derived from Figures 2 and 3 that the pressure drop within the horizontal section is roughly two times larger than in the vertical section. The higher pressure drop results from

the higher quality, hence an increased two-phase friction factor, which is caused by the needle valve's heat leak and by heat transfer through the MLI along the horizontal section. Since the riser is almost completely immersed in the LHe mobile dewar, the heat leak to the LHe flow is negligible. The pressure drop along the needle valve was not modeled. Both figures above show that the pressure drop derived from the homogeneous model deviates by 24% in terms of the mean absolute percentage error from the experimental data. For the riser section the homogeneous model reproduces the experimental data more accurately (13%).

Due to the rather poor agreement by the homogeneous model two other pressure drop correlations by [6] and [7] were considered. The respective results are presented in Figures 4 and 5. Since the model by [6] was developed for a non-adiabatic LHe flow through a narrow channel of 1.6 mm at $G = 100$ to 400 kg/(m² s) it reproduces the push mode data with $G > 170$ kg/(m² s) best, with an accuracy of 18%. In the pull mode the deviation is larger than for the homogeneous model (35%), although [6] gave a correlation for subatmospheric pressures and $G = 30$ to 180 kg/(m² s), too. For $G < 100$ kg/(m² s) the model by [7] agrees fairly well with the experimental data (13%), but at higher mass fluxes the deviation is the highest of all considered models. The deviations of the model by [7] are mainly caused by the use of the Blasius friction factor instead of the Colebrook one by the two other models. Using the Colebrook equation with the model by [7] results in far too high pressure drops. Since this model is based on a separated flow approach, it should be considered as inappropriate for LHe transfer lines. All models are rather sensitive to the assumed distribution of the heat flux along the transfer line.

It must be stated that the calculated heat leak is around 0.9 W, which is 45% less than the measured value of 1.65 W [1]. This deviation is mainly caused by uncertainties regarding the calculations of the heat transfer along the needle valve and through the MLI. The MLI is hand-wrapped around the inner tube causing variations of the layer density along different transfer lines and even along the horizontal section of one single line. Furthermore, the correlation published by [13] has an uncertainty of $\pm 80\%$, emphasizing the difficulties of calculating MLI heat transfer accurately. Nevertheless, the respective correlation is still the most accurate one for the considered MLI type.

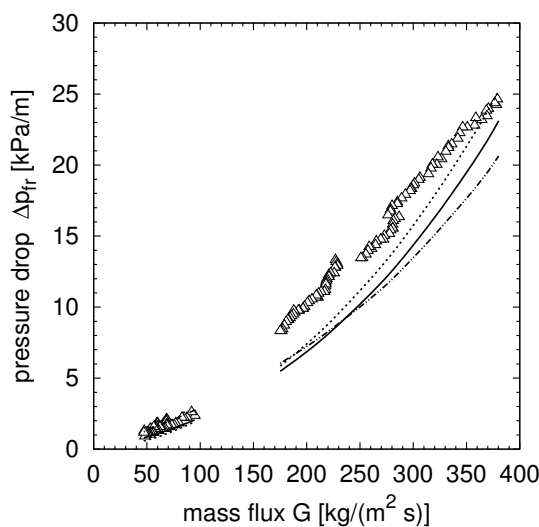


Figure 4. Frictional pressure drop per unit length; $(p_2 - p_3)_{fr}$ (Δ), homogeneous model (—), [6] (---), [7] (— · —).

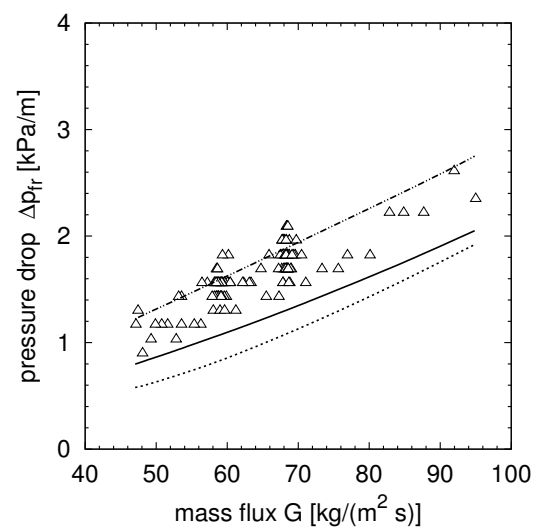


Figure 5. Frictional pressure drop at low values of G ; $(p_2 - p_3)_{fr}$ (Δ), homogeneous model (—), [6] (---), [7] (— · —).

In addition to the hydraulic characteristics of the LHe flow, the thermohydraulic model aims to cover the heat transfer parameters, too. Assuming an isobaric heat input and an isenthalpic throttling of the flow due to the several pressure drop terms, the quality at the transfer line outlet can be estimated. The resulting values of x_{out} are shown in Figure 6.

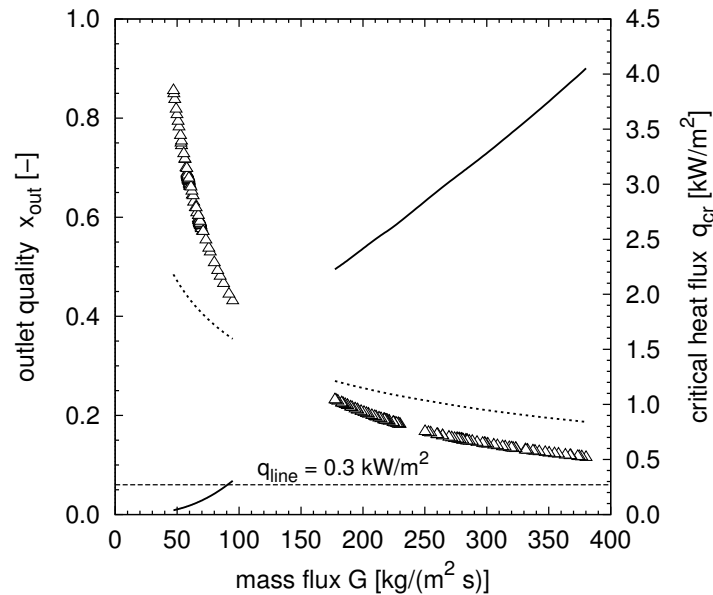


Figure 6. Outlet quality and critical heat flux; x_{out} (Δ), x_{lim} according to [6] (- - -), q_{cr} according to [6] (—).

During pull mode the outlet quality varies between 0.43 ($G = 95 \text{ kg}/(\text{m}^2 \text{ s})$) and 0.86 ($G = 47 \text{ kg}/(\text{m}^2 \text{ s})$), which is in correspondence with a measured value of $x = 0.55$ for $G = 70 \text{ kg}/(\text{m}^2 \text{ s})$ derived by means of an electrical heater. For $G = 40 \text{ kg}/(\text{m}^2 \text{ s})$ the complete flow evaporates inside the transfer line (see [1]). Subbotin et al. found that the critical heat flux rapidly decreases if a limiting quality x_{lim} is exceeded. It can be derived from Figure 6 that this is the case for the complete mass flux range in pull mode. Due to the high quality at low mass fluxes, the critical heat flux is exceeded, which may lead to onset of film boiling. The actual heat flux to the transfer line was measured to be $0.3 \text{ kW}/\text{m}^2$ [1]. At outlet qualities below 0.2 the calculated critical heat flux is larger than $2.2 \text{ kW}/\text{m}^2$.

In the case of a LHe transfer line the thermal resistance of the MLI predominates the heat transfer characteristics of the complete assembly, $R_{MLI}/R_{tube} \approx 10^4$. As a result, the overall heat flux is rather insensitive to the heat transfer coefficient of the LHe flow. Therefore, no specific heat transfer correlation valid for a mini- or micro-channel assembly was implemented.

6. Conclusion

A thermohydraulic model was developed to calculate the pressure drop and heat leak of LHe flowing through a transfer line with a narrow inner diameter. It was shown that the pressure drop correlation by Subbotin et al. reproduces the experimental data best, with a mean absolute percentage error of $\pm 22\%$. The thermohydraulic model shows that during pull mode, i.e. at low mass fluxes and high qualities the actual heat leak is larger than the critical heat flux, resulting in a boiling crisis during the transfer. Nevertheless, the homogeneous model gives fairly good results for a first estimation of the overall pressure drop in the system. On basis of the existing model several parameters like the insulation and the hydraulic design will be modified virtually to find a transfer line design with reduced transfer losses.

Acknowledgments

This work was financially supported by the Federal Ministry of Economics and Technology on the basis of a decision by the German Bundestag.

References

- [1] Dittmar N, Welker D, Haberstroh Ch, Hesse U and Krzyzowski M 2015 *IOP Conf. Ser.: Mater. Sci. Eng.* **101** 012097
- [2] Regier C, Pieper J and Matias E 2011 *Cryogenics* **51** pp 1-15
- [3] Veeramani C and Spiteri R J 2013 *Applied Mathematical Modelling* **37** pp 34-49
- [4] Huang X and Van Sciver S W 1995 *Cryogenics* **35** pp 467-74
- [5] Nakagawa S et al. 1984 *Proc. 10th ICEC* (Guildford: Butterworth) pp 570-73
- [6] Subbotin V I et al. 1985 *Cryogenics* **25** pp 261-65
- [7] Kim S-M and Mudawar I 2014 *International Journal of Heat and Mass Transfer* **77** pp 74-97
- [8] Lockhart R W and Martinelli R C 1949 *Chemical Engineering Progress* **45** pp 39-48
- [9] Ghiaasiaan M 2008 *Two-phase flow, boiling and condensation. In conventional and miniature systems* (Cambridge: Cambridge University Press)
- [10] Colebrook C F 1939 *Journal of the ICE* **11** pp 133-56
- [11] Deev V I, Gordeev V, Pridantsev A I, Petrovichev V I and Arkhipov V V 1977 *Atomic Energy* **42** pp 381-83
- [12] Berman T L, Lavine A S, Incropera F P and DeWitt D P 2011 *Fundamentals of Heat and Mass Transfer 7th Edition* (Hoboken: Wiley)
- [13] Cunnington G R, Keller C W and Bell G A 1971 *Thermal performance of multilayer insulations* (Cleveland: NASA)
- [14] Collier J G and Thome J R 1994 *Convective boiling and condensation* (Oxford: Clarendon Press)
- [15] Barron R F 1999 *Cryogenic Heat Transfer* (New York: Taylor and Francis)
- [16] Ogata H and Sato S 1974 *Cryogenics* **14** pp 375-80
- [17] Wallis G B 1969 *One-dimensional Two-phase Flow* (New York: McGraw-Hill Inc.)
- [18] Dittmar N, Haberstroh Ch, Hesse U and Krzyzowski M 2016 *Cryogenics*